Conformational and Functional Study of Magainin 2 in Model Membrane Environments Using the New Approach of Systematic Double-D-Amino Acid Replacement

Torsten Wieprecht, Margitta Dathe,* Michael Schümann, Eberhard Krause, Michael Beyermann, and Michael Bienert

Forschungsinstitut für Molekulare Pharmakologie, Alfred-Kowalke-Strasse 4, D-10315 Berlin, Germany

Received February 14, 1996; Revised Manuscript Received May 15, 1996[⊗]

ABSTRACT: Systematic double-D-amino acid replacement of adjacent amino acids has been used to study the secondary structure of the amphiphilic, antibiotic peptide magainin 2 amide (M2a) by circular dichroism spectroscopy. Bound to liposomes, the secondary structure of the peptide is characterized by a weak α-helix in the N-terminus and a stable α-helix between residues 9 and 21. The lack of conformational differences in the peptide when bound to vesicles of varying negative charge density indicates marked independence of the structure from electrostatic forces. The similarity of the helicity profiles observed for double D-isomers bound to vesicles and in the presence of sodium dodecyl sulfate micelles (SDS) clearly shows that SDS can mimic magainin−lipid interactions. In contrast, in 1:1 trifluoroethanol/buffer (v/v), the peptide exhibits a weak α-helix extended from the N- to the C-terminus. Dye release experiments from vesicles of phosphatidylglycerol showed that double-D-amino acid substitution only in the region of the stable helix results in a reduction of the membrane-permeabilizing ability. On vesicles with a reduced amount of acidic phospholipids, double-D-amino acid substitution in any position leads to a drastic reduction of peptide-induced membrane permeabilization. Whereas the activity of M2a on phosphatidylglycerol was found to be mainly electrostatically determined, hydrophobic interactions play a decisive role in the interaction with vesicles of reduced negative charge density. Fluorescence investigations of tryptophan-containing analogs of high and low helicity showed that differences in the location of the chromophores of the membrane-bound peptides do not exist.

The magainins are a class of positively charged peptides isolated from the skin of the African clawed frog *Xenopus laevis* (Zasloff, 1987). Peptides in this group show a broad spectrum of antibacterial, antifungal, and tumoricidal activity, but they are not hemolytic (Zasloff, 1987; Zasloff et al., 1988; Soravia et al., 1988) and therefore represent potential candidates for the development of drugs. Magainins have the ability to adopt an amphiphilic α-helical conformation and are hence membrane active (Chen et al., 1988). Their net positive charge seems to be important for interaction with negatively charged membrane phospholipids (Matsuzaki et al., 1991; Vaz Gomes et al., 1993). The magainins have been shown to act directly by enhancing membrane permeability (Westerhoff et al., 1989; Matsuzaki et al., 1989, 1991; Juretic et al., 1994). In planar lipid bilayers, magainins form voltage-gated ion channels with a broad range of conductance levels (Duclohier et al., 1989; Cruciani et al., 1992). However, the detailed mechanism of action is yet unclear, and different opinions exist as to whether the enhancement of membrane permeability is due to the formation of water-filled pores or the result of an overall disturbance of the structure of the lipid bilayer (Grant et al., 1992; Matsuzaki et al., 1995a).

Several conformational investigations of magainin 1 and 2 in different solvent systems and in the presence of lipid bilayers have been carried out using circular dichroism (CD),[1] nuclear magnetic resonance (NMR), Raman, or Fourier transform infrared (FT-IR) spectroscopy. In water, the peptides have been shown to be conformationally flexible (Marion et al., 1988). In more hydrophobic 2,2,2-trifluoroethanol (TFE)/water solutions, the conformation of magainin 1 and 2 is partially α-helical, with a helical content between 25 and 35% as determined from CD spectra (Chen et al., 1988; Bessalle et al., 1992). A mainly α-helical structure in 25% TFE has been suggested on the basis of ^{1}H NMR investigations (Marion et al., 1988).

Likewise, in the presence of sodium dodecyl sulfate micelles (SDS) and lipid vesicles, magainin 1 and 2 have been reported to exist mainly in α-helical conformations (Duclohier et al., 1989; Matsuzaki et al., 1989, 1991; Williams et al., 1990; Jackson et al., 1992). Investigations with vesicles and oriented bilayers led to the conclusion that at high and moderate lipid:peptide ratios the peptides are oriented perpendicular to the bilayer normal with the hydrophilic side chains exposed to the phospholipid head groups and the hydrophobic side chains penetrating into the acyl chain region (Bechinger et al., 1993; Matsuzaki et al., 1994). Raman studies showed that liposome-associated magainin 2 amide exhibits about 58% helicity on negatively charged 1,2-dimyristoylphosphatidyl-DL-glycerol (DMPG)

* Author to whom correspondence should be addressed.

[⊗] Abstract published in *Advance ACS Abstracts,* August 1, 1996.

[1] Abbreviations: CD, circular dichroism; NMR, nuclear magnetic resonance; FT-IR, Fourier transform infrared; TFE, 2,2,2-trifluoroethanol; SDS, sodium dodecyl sulfate; M2a, magainin 2 amide; LUVs, large unilamellar vesicles; SUVs, small unilamellar vesicles; POPC, 1-palmitoyl-2-oleoylphosphatidylcholine; POPG, 1-palmitoyl-2-oleoylphosphatidyl-DL-glycerol; SD, standard deviation; Tris, tris(hydroxymethyl)aminomethane; DMPC, 1,2-dimyristoylphosphatidylcholine; DMPG, 1,2-dimyristoylphosphatidyl-DL-glycerol.

S0006-2960(96)00362-5 CCC: $12.00

Table 1: Peptides of the Double-D-Amino Acid Replacement Set

peptide sequence[a]																						peptide designation
1	2	3	4	5	6	7	8	9	10	11	12	13	14	15	16	17	18	19	20	21	22	23	
G	I	G	K	F	L	H	S	A	K	K	F	G	K	A	F	V	G	E	I	M	N	S	M2a
G	*i*	G	*k*	F	L	H	S	A	K	K	F	G	K	A	F	V	G	E	I	M	N	S	i^{2},k^{4} M2a
G	I	G	*k*	*f*	L	H	S	A	K	K	F	G	K	A	F	V	G	E	I	M	N	S	k^{4},f^{5} M2a
G	I	G	K	*f*	*l*	H	S	A	K	K	F	G	K	A	F	V	G	E	I	M	N	S	f^{5},l^{6} M2a
G	I	G	K	F	L	*h*	*s*	A	K	K	F	G	K	A	F	V	G	E	I	M	N	S	h^{7},s^{8} M2a
G	I	G	K	F	L	H	S	*a*	*k*	K	F	G	K	A	F	V	G	E	I	M	N	S	a^{9},k^{10} M2a
G	I	G	K	F	L	H	S	A	K	*k*	*f*	G	K	A	F	V	G	E	I	M	N	S	k^{11},f^{12} M2a
G	I	G	K	F	L	H	S	A	K	K	*f*	G	*k*	A	F	V	G	E	I	M	N	S	f^{12},k^{14} M2a
G	I	G	K	F	L	H	S	A	K	K	F	G	K	*a*	*f*	V	G	E	I	M	N	S	a^{15},f^{16} M2a
G	I	G	K	F	L	H	S	A	K	K	F	G	K	A	*f*	*v*	G	E	I	M	N	S	f^{16},v^{17} M2a
G	I	G	K	F	L	H	S	A	K	K	F	G	K	A	F	*v*	G	*e*	I	M	N	S	v^{17},e^{19} M2a
G	I	G	K	F	L	H	S	A	K	K	F	G	K	A	F	V	G	E	*i*	*m*	N	S	i^{20},m^{21} M2a
G	I	G	K	F	L	H	S	A	K	K	F	G	K	A	F	V	G	E	I	M	*n*	*s*	n^{22},s^{23} M2a

[a] The one-letter code for amino acids is used. Capital letters refer to L-amino acids and small letters to D-amino acids. In the case of glycine, the two neighboring residues are replaced by their D-enantiomers.

vesicles while the helicity is reduced when bound to zwitterionic 1,2-dimyristoyl phosphatidylcholine (DMPC) vesicles (Williams et al., 1990). CD investigations with small unilamellar vesicles (SUVs) composed of a variety of phospholipids revealed an α-helix content between 68 and 85% for magainin 1 and 2 (Matsuzaki et al., 1991). On the basis of these observations and the fact that a C-terminal-truncated magainin shows a similar affinity to egg PG vesicles, it has been suggested that the C-terminal part of magainin is nonhelical and expelled from the bilayer (Matsuzaki et al., 1991, 1993). Furthermore, an α-helical conformation with some β-structure has been reported for magainin 2 amide on DMPG vesicles using FT-IR spectroscopy (Jackson et al., 1992). In contrast, ^{15}N solid-state NMR studies of magainin 2 in oriented bilayers suggested that nearly the entire peptide is α-helical (Bechinger et al., 1993). These results demonstrate the variety of current opinions regarding the helical content of membrane-bound magainins and the location of the helix. Since the amphiphilic α-helix is believed to be the main structural feature responsible for membrane activity, a precise determination of the helical domains is important. Moreover, analysis of the structural differences of magainins bound to vesicles of different phospholipids, especially to vesicles of different surface charge, would appear to be an important prerequisite for an understanding of peptide−membrane interactions.

The method of choice for determination of detailed peptide secondary structure is two-dimensional ^{1}H NMR spectroscopy in solution. Unfortunately, peptides associated to lipid vesicles cannot be investigated by this method because of slow molecular reorientation rates. SDS micelles are therefore often used to mimic the bilayer environment (Rizo et al., 1993; Franklin et al., 1994; Gilbert & Baleja, 1995), but the conformational identity of the peptide bound to SDS micelles and phospholipid vesicles must be established. In contrast, CD, Raman, and FT-IR spectroscopy are useful methods for investigation of peptide structure in the vesicle-bound state. However, these methods provide information only regarding the overall content of secondary structures without allowing location of these structural elements.

In order to locate the α-helical regions of the C-terminal-amidated magainin 2 (M2a) bound to phospholipid vesicles and in membrane-mimetic environments such as SDS micellar solutions and TFE/buffer mixtures, we studied by CD spectroscopy a set of peptides with a pairwise substitution of adjacent amino acids by their D-enantiomers (double D-isomers, see Table 1). D-Amino acid substitution was found to destabilize helical regions without changing other properties of the peptide such as hydrophobicity, side chain functionality, or charge distribution (Fairman et al., 1992; Pouny & Shai, 1992). However, the resulting conformational effect of a single D-substitution is not always pronounced enough for reliable determination (Fairman et al., 1992; Krause et al., 1995). The replacement of two adjacent amino acids by their D-isomers has been shown to induce a more pronounced disturbance of the local conformation. It was shown that the degree of structural disturbance of an α-helix due to a double-D-amino acid substitution correlates positively with the helicity of the replaced region in the all-L-amino acid peptide (Krause et al., 1994, 1995). In other words, replacement near the center of a stable helix decreases the overall helicity significantly, whereas double-D-amino acid substitution in a more flexible helical region (e.g. at the ends of a helix, where not all CO or NH groups are hydrogen bonded) has only a moderate influence on the helicity. Double-D-amino acid replacement in a nonhelical region is not expected to influence the overall helical content of the peptide. The conformational disturbance is quantified by the change in the CD spectrum of the double D-analogs relative to that of the unsubstituted peptide. Recently, this method has been used to localize the helical domains of neuropeptide NPY and amphiphilic model peptides in a TFE/water mixture (Krause et al., 1995; Rothemund et al., 1995). Furthermore, we used the systematic double-D-amino acid replacement of adjacent amino acids to investigate the role of different peptide regions in membrane permeabilization. We studied the ability of M2a and the double D-isomers to release dye from large unilamellar vesicles (LUVs) of different negative surface charge and were able to determine the peptide regions which are important for enhancing membrane permeability. Additionally, fluorescence measurements of tryptophan-containing analogs were used to study the environment of the hydrophobic residue in the lipid-bound state.

EXPERIMENTAL PROCEDURES

Materials. All lipids were purchased from Avanti Polar Lipids, Inc., Alabaster, AL. Calcein was obtained from Fluka Chemie, Neu-Ulm, Germany, tris(hydroxymethyl)aminomethane (Tris) from Merck KGaA, Darmstadt, Germany,

and trifluoroethanol from Aldrich-Chemie, Steinheim, Germany, and the Fmoc amino acids were from Novabiochem, Bad Soden, Germany. All other chemicals were of reagent grade.

Peptide Synthesis. Peptides were synthesized automatically by solid-phase methods using standard Fmoc chemistry on Tenta Gel S RAM resin (0.21 mmol/g; RAPP Polymere, Tübingen, Germany) in the continuous flow mode on a MilliGen 9050 peptide synthesizer (Beyermann et al., 1992). Purification was carried out by preparative HPLC on PolyEncap A300, 10 μm (250 $\times$ 20 mm inside diameter) (Bischoff Analysentechnik), to give final products >95% pure by HPLC analysis. All peptides were characterized by matrix-assisted laser desorption ionization mass spectrometry (MALDI II; Kratos, Manchester, U.K.) with the peptide content of lyophilized samples being determined by quantitative amino acid analysis (Biotronik-Eppendorf LC 3000 instrument).

Small Unilamellar Vesicle Preparation. The lipid film was dried overnight under high vacuum and then suspended by vortex mixing in buffer [10 mM Tris, 154 mM NaCl, and 0.1 mM EDTA (pH 7.4)] to give a final lipid concentration between 20 and 40 mM. The suspension was sonicated (under nitrogen, in ice−water) for 25 min using a titanium tip ultrasonicator. Titanium debris was removed by centrifugation. Dynamic light-scattering experiments confirmed the existence of a main population of vesicles (more than 95% mass content) with a mean diameter of 46 $\pm$ 1 nm. The polydispersity index was 0.3.

Large Unilamellar Vesicle Preparation. After the dried lipid was vortexed in calcein buffer solution [70 mM calcein, 10 mM Tris, and 0.1 mM EDTA (pH 7.4)], the suspension was freeze−thawed in liquid nitrogen for seven cycles and extruded through polycarbonate filters (Hope et al., 1985) (six times through two stacked 0.4 μm pore size filters followed by eight times through two stacked 0.1 μm pore size filters). Untrapped calcein was removed from the vesicles by gel filtration on a Sephadex G75 column [eluent, buffer containing 10 mM Tris, 154 mM NaCl, and 0.1 mM EDTA (pH 7.4)]. Lipid concentration was determined by phosphorus analysis (Böttcher et al., 1961).

Noncovalent Immobilized Artificial Membrane Chromatography. The retention behavior of peptides was studied on a DMPC-loaded Vydac C18 column (Vydac 218TP5415; 150 $\times$ 4.6 mm inside diameter). The column was prepared by noncovalent immobilization of DMPC on the reversed-phase column by pumping 10 mL of a solution prepared from 20 mg/mL DMPC in 2-propanol/water, 1.5:8.5, through the column. The surface density of DMPC was determined from the breakthrough curves of the lipid solution to be 1.95 μmol/m^2 which is close to the lipid density of bilayer systems and confirms the formation of a bilayer-like structure with the C18 chains of the stationary phase. The stability of the DMPC loading was measured at pH 2.0 (0.1% TFA) and pH 7.0 (0.07 M KH_2PO_4) and found to be appropriate in elution systems containing less than 35% of acetonitrile. This allows determination of partition coefficients (retention times) of peptides (E. Krause, unpublished results).

Chromatographic measurements were performed on a Shimadzu LC-10A gradient HPLC system consisting of two LC-10AD pumps, an SIL-10A autoinjector, and an SPD-M10A detector operating at 215 nm. The sample concentration was 1 mg/mL peptide in eluent A with an injection volume of 20 μL. Separations were performed at 25 °C (thermostatted system) and at an eluent flow rate of 1 mL/min. Mobile phases A and B consisted of 0.07 M KH_2PO_4 in water, at pH 7.0, and 0.07 M KH_2PO_4 in 35% acetonitrile/65% water (v/v), at pH 7.0, respectively. Retention times of the peptides were determined using a linear gradient of 1 to 90% B in 40 min.

Circular Dichroism Measurements. CD measurements of the peptide solutions were carried out on a Jasco 720 spectrometer between 185 and 260 nm in TFE and SDS solution and between 200 and 260 nm in a vesicle suspension at 23 °C if not otherwise noted. Minor contributions of circular dichroism and differential scattering of the SUVs were eliminated by subtracting the lipid spectra of the corresponding peptide-free suspensions. Absorption flattering was found to be negligible up to a lipid concentration of 15 mM. The helicity of the peptides was determined from the mean residue ellipticity [Θ] at 222 nm (Chen et al., 1972) or by curve fitting to reference protein spectra using the CONTIN algorithm (Provencher, 1982) and the VARSLC program (Toumadje, personal communication). The reported helicities are the mean of two independent experiments. The error of all methods was 5% helicity.

Binding Isotherms. CD-derived binding isotherms were determined from the changes of the CD of peptide solutions (three different concentrations between 5×10^{-5} and 5×10^{-6} M) after adding different amounts of SUVs. For determination of binding isotherms, the following relations were used:

$$\text{(a) } F = \Theta_{222}(0) - \Theta_{222}$$

where F is the relative signal, $\Theta_{222}(0)$ the ellipticity in the absence of lipid, and Θ_{222} the measured ellipticity in the presence of lipid, and

$$\text{(b) } F = F_\infty(c_B/c_P) = F_\infty(c_L/c_P) \times r$$

where F_∞ is F of the completely bound peptide, c_L the lipid concentration, c_P the total peptide concentration, c_B the lipid-bound peptide concentration, and $r = c_B/c_L$. From these equations and the mass conservation equation, the binding isotherm can be evaluated [for a detailed description, see Schwarz and Beschiaschvili (1989)]. Binding isotherms from calcein-releasing experiments were derived according to Matsuzaki et al. (1989).

Calcein Release Assay. Aliquots of the vesicular suspension (10−20 μL) were injected into a cuvette containing 2.5 mL of a stirred peptide solution at 23 °C. Calcein release from LUVs was determined fluorometrically by measuring the decrease in self-quenching (excitation at 490 nm, emission at 520 nm) on a Perkin-Elmer LS 50B spectrofluorometer. The fluorescence intensity corresponding to 100% release was determined by addition of 100 μL a of 10% Triton X-100 solution.

Fluorescence Measurements. Fluorescence measurements of the tryptophan-containing analogs W^{16} M2a and a^{15},w^{16} M2a were performed on a Perkin-Elmer LS 50B spectrofluorometer at 23 °C. Emission spectra were recorded between 300 and 450 nm (excitation wavelength of 280 nm) using a peptide concentration of 2 μM in buffer [10 mM Tris, 154 mM NaF, and 0.1 mM EDTA (pH 7.4)] or in a 400 μM SUV suspension. Emission was observed using a

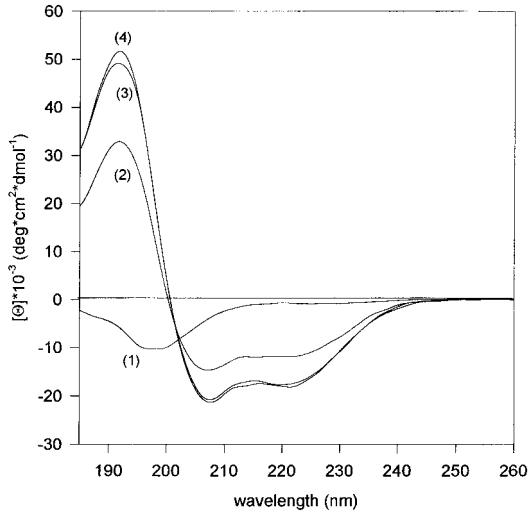

FIGURE 1: CD spectra of M2a (25 μM) in (1) buffer [10 mM Tris, 154 mM NaF, and 0.1 mM EDTA (pH 7.4)], (2) 1:4 TFE/buffer (v/v), (3) 1:1 TFE/buffer (v/v), and (4) 4:1 TFE/buffer (v/v). The development of intensive negative bands at 222 and 209 nm points to a transition from a random to an α-helical structure with increasing TFE contents.

290 nm red edge filter. The contribution of light scattering caused by SUVs was corrected by subtracting the spectra of the SUV suspension containing the corresponding nonfluorescent peptide.

The abilities of cesium ions and iodide ions to quench the tryptophan fluorescence (emission at 350 nm, 15 nm slit width) of the peptides in buffer and in lipid suspensions were studied by addition of increasing amounts of the quenchers (stock solutions, 4 M potassium iodide containing 1 mM $Na_2S_2O_3$ and 4 M cesium chloride; peptide and lipid concentrations were the same as in the emission spectra). The quenching constants were evaluated from the Stern−Volmer plots I_0/I via $c_{quencher}$ (I_0 is the fluorescence intensity in the absence of a quencher, I the fluorescence intensity in the presence of the quencher, and $c_{quencher}$ the concentration of the quencher).

RESULTS

Structure in TFE. The CD spectra of magainin 2 amide in Tris buffer saline and after addition of TFE are shown in Figure 1. The intense negative bands at 222 and 209 nm reflect the transition from a flexible structure to a helical conformation in the presence of TFE. The helical content in 1:1 TFE/buffer (v/v), calculated by three different methods, ranges between 50 and 55% (Table 2). Double-D-amino acid substitution at any position reduces the helicity by 15−34% compared with M2a (Figure 2A), revealing that all substitutions disturb the α-helix. On the basis of the helicity profile, a completely helical peptide chain is suggested. Typically, a minimum in helicity is expected as a result of double-D-amino acid substitution in the center of a stable helix, whereas helicity should be less decreased as a result of substitution at the helix ends where the conformational flexibility is higher (Chakrabartty et al., 1991; Krause et al., 1995). The profile observed for the magainin replacement set does not show a pronounced minimum and is (except n^{22},s^{23} M2a and v^{17},e^{19} M2a) little differentiated. Both observations, the replacement profile and the calculated helicity of about 50%, lead to the conclusion that the α-helix of M2a in 1:1 TFE/buffer (v/v) is weak and flexible. This can be understood by a time-averaged helical probability of about 50% for each of the amino acid positions. To confirm this conclusion, the double-D-amino acid replacement set was investigated at a reduced temperature (1 °C) (Figure 2B). As expected, the helicity of M2a was significantly enhanced to 78% and the profile of the double D-isomers shows a pronounced minimum for f^{16},v^{17} M2a and v^{17},e^{19} M2a, suggesting that the helix is most stable in this region.

Binding of Peptides to POPG, POPC/POPG (3:1), and POPC Vesicles. We investigated M2a and the double-D-

Table 2: Percentage of α-Helicity of M2a in Buffer and TFE/Buffer Mixtures[a]

solvent	α-helicity (%)		
	$[\Theta]_{222}$[b]	CONTIN[c]	VARSLC[d]
buffer	0	0	0
1:4 TFE/buffer (v/v)	31	37	37
1:1 TFE/buffer (v/v)	50	55	55
4:1 TFE/buffer (v/v)	52	57	57

[a] All CD data were obtained at 23 °C, pH 7.4, and a peptide concentration of 25 μM. [b] Helical content was calculated from $[\Theta]_{222}$ according to Chen et al. (1972). [c] Helical content as obtained by curve fitting with reference protein spectra using the CONTIN algorithm. [d] Helical content as calculated by curve fitting using the VARSLC program.

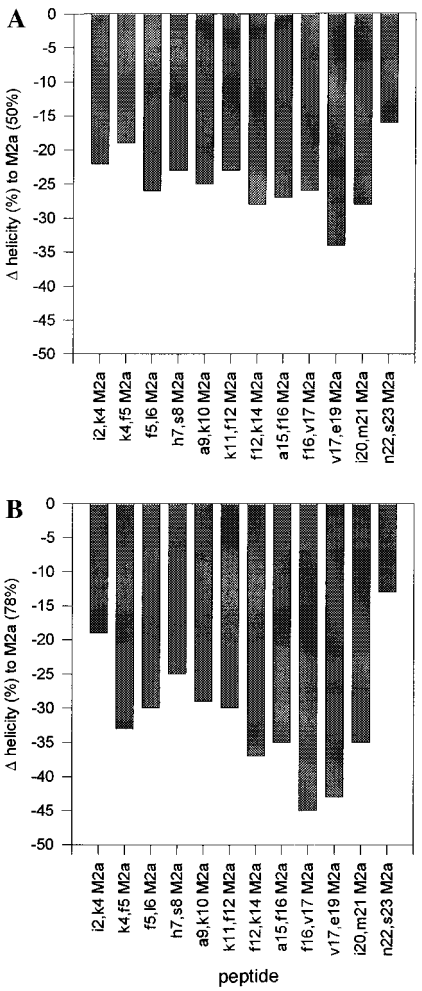

FIGURE 2: Helicity profiles of the double-D-amino acid replacement set (change of helicity compared to M2a) in 1:1 TFE/buffer (v/v) at (A) 23 °C and (B) 1 °C (50 μM peptide). Helical content was estimated from $[\Theta]_{222}$ as described in Experimental Procedures.

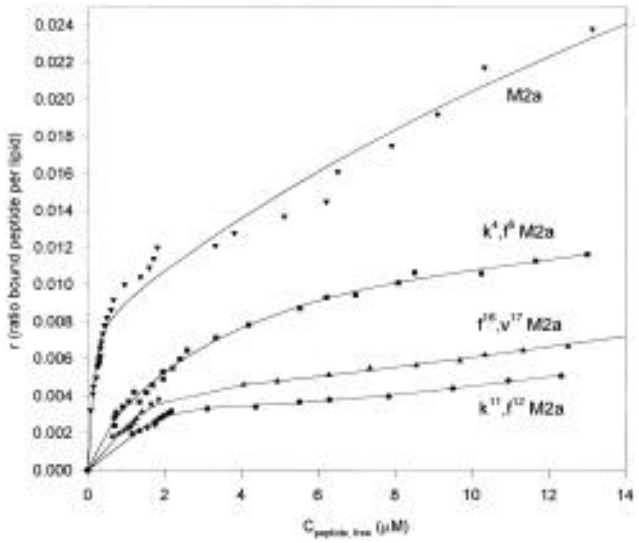

FIGURE 3: Binding isotherms (23 °C) of M2a, k^4,f^5 M2a, k^{11},f^{12} M2a, and f^{16},v^{17} M2a on POPC/POPG (3:1) SUVs. Isotherms were derived by titration of three different peptide concentrations with vesicle suspensions.

amino acid replacement set on three types of vesicles: negatively charged 1-palmitoyl-2-oleoylphosphatidyl-DL-glycerol (POPG) vesicles, POPC/POPG (3:1, mole/mole) vesicles of moderate negative surface charge, and electrically neutral 1-palmitoyl-2-oleoylphosphatidylcholine (POPC) vesicles. For evaluation of the CD spectra of peptide/lipid mixtures, it must be taken into consideration that the measured CD is the sum of the contributions of the lipid-bound and the free peptide. Therefore, for the study of the conformation of the lipid-bound fraction, it is necessary to choose conditions with a negligible free peptide concentration. Binding isotherms of four representative peptides to POPG, mixed POPC/POPG (3:1), and POPC vesicles were determined to calculate appropriate peptide and lipid concentrations. The binding isotherms of M2a and the double D-isomers bound to POPC/POPG (3:1) and POPC SUVs were derived using CD spectroscopy by titration of peptide solutions with vesicle suspensions (Schwarz & Beschiaschvili, 1989) [isotherms on POPC/POPG (3:1); Figure 3]. Isotherms of the peptides bound to POPG vesicles were determined by analyzing the peptide- and lipid-concentration dependency of calcein leakage from LUVs (Matsuzaki et al., 1989) (isotherms not shown). The apparent binding constants evaluated from the linear range of the binding isotherms are listed in Table 3. As expected, the affinity of the investigated peptides significantly decreases with reduction of the negative surface charge of the vesicles.

On the basis of the binding isotherms, we selected conditions (Table 3) for the subsequent structure investigations in POPG and POPC/POPG (3:1) vesicle suspensions with at least 95% lipid-bound peptide. Consequently, the measured CD can be interpreted as the CD of the vesicle-bound peptides. Unfortunately, corresponding conditions for the investigations on zwitterionic POPC vesicles could not be found due to the low affinity of the double D-isomers for these vesicles.

Structure of Magainin 2 Amide on POPG and POPC/POPG SUVs. Binding of M2a to POPG and POPC/POPG (3:1) SUVs leads to a transition from a random coil structure to a helical conformation with a helicity of 76 and 75%, respectively. The double-D-amino acid replacement profile for peptides bound to POPG SUVs (Figure 4A) reflects a decrease in helicity for all of the isomers investigated. The much more pronounced decreases observed for the isomers a^9,k^{10} M2a to i^{20},m^{21} M2a lead to the suggestion that in this region a very stable, well-developed α-helix exists. In contrast, the moderate reduction in helicity observed for i^2,k^4 M2a, k^4,f^5 M2a, f^5,l^6 M2a, and h^7,s^8 M2a indicates that the N-terminal region up to position 8 exhibits a less stable helix.

A reduction of the negative surface charge in POPC/POPG (3:1) liposomes compared to the exclusively acidic POPG vesicles reduces the influence of electrostatic interactions on peptide binding. However, the helicity profile of peptides bound to POPC/POPG (3:1) SUVs (Figure 4B) remains almost unchanged when compared with the POPG profile (Figure 4A). Obviously, the structural properties of the membrane-bound M2a are identical.

Magainin 2 Amide Bound to POPC SUVs. Because the double D-isomers have been found to exhibit a very low affinity for POPC vesicles (see K_{app}, Table 3), the peptides were not completely bound during the CD investigations. We used an indirect method to determine the fraction of bound peptide. Assuming that the structure of the bound peptide is independent of the amount of negatively charged phospholipids, the secondary structure of M2a as well as that of the double D-isomers can be expected to be identical when bound to POPC, POPG, and POPC/POPG (3:1) SUVs. The helicity of peptides bound to negatively charged vesicles is known (Figure 4). Hence, the amount of POPC-bound peptide under the conditions used can be evaluated from the equation $X_{bound} = \Theta_{222}(POPC)/\Theta_{222}(POPC/POPG)$, where X_{bound} is the bound peptide fraction, $\Theta_{222}(POPC)$ the measured ellipticity in the presence of POPC SUVs (not shown), and $\Theta_{222}(POPC/POPG)$ the ellipticity of the peptides completely bound to POPC/POPG (3:1) SUVs. If the assumption of identical structural properties of M2a bound at POPC and POPC/POPG (3:1) vesicles is valid, the resulting binding profile [X_{bound} compared to X_{bound}(M2a)] (Figure 5A) should reflect the individual apparent binding constants of the peptides.

To confirm our assumption, we determined the retention times of the double-D-amino acid replacement set by non-covalent immobilized artificial membrane chromatography on a DMPC-loaded Vydac C18 column. The retention time of a substance is known to be proportional to its partition coefficient (or the binding constant) between the aqueous mobile phase and the stationary phase for a given chromatographic system. The profile of the retention times of M2a and the double D-isomers is given in Figure 5B. The excellent correlation of the CD-derived binding profile (Figure 5A) and the retention time profile (Figure 5B) confirms that the assumption of identical structural properties of M2a bound at POPC, POPG, and POPC/POPG (3:1) liposomes is valid. Thus, also on POPC vesicles, M2a seems to form a weak helix from the N-terminus up to position 8 and a well-developed, strong helix in the sequence from 9 to 21.

Structure in SDS Micelles. The influence of double-D-amino acid substitution on the structural properties of M2a in the presence of SDS micelles is shown in Figure 6. As found for the different vesicles, double-D-amino acid replacement up to position h^7,s^8 has little effect on the peptide helicity whereas a more pronounced decrease is found for

Table 3: Apparent Binding Constants (K_{app}) of M2a and Double D-Isomers[a]

peptide	K_{app} (M^{-1}) of POPG [b]	bound peptide fraction (%)[c]	K_{app} (M^{-1}) of POPPC/POPG (3:1)[d]	bound peptide fraction (%)[e]	K_{app} (M^{-1}) of POPC[d]
M2a	195 000	>99	20000	>99	400
k^4,f^5 M2a	260 000	>99	2500	97	73
k^{11},f^{12} M2a	130 000	>99	1500	95	32
f^{16},v^{17} M2a	76 000	>99	2200	97	37

[a] Apparent binding constants were evaluated from the linear range of the binding isotherms. [b] Binding isotherms were obtained by calcein release from LUVs. Control experiments employing SUVs revealed only slight differences in membrane activity of the peptides. [c] Calculated from the binding constants and peptide and POPG concentrations of 50 μM and 13.0 mM, respectively, which were used for secondary structure determination of the lipid-bound peptides. [d] Binding isotherms were obtained as described in Figure 3. [e] Calculated from the binding constants and peptide and POPC/POPG (3:1) concentrations of 25 μM and 13.7 mM, respectively, which were used for secondary structure determination of the lipid-bound peptides.

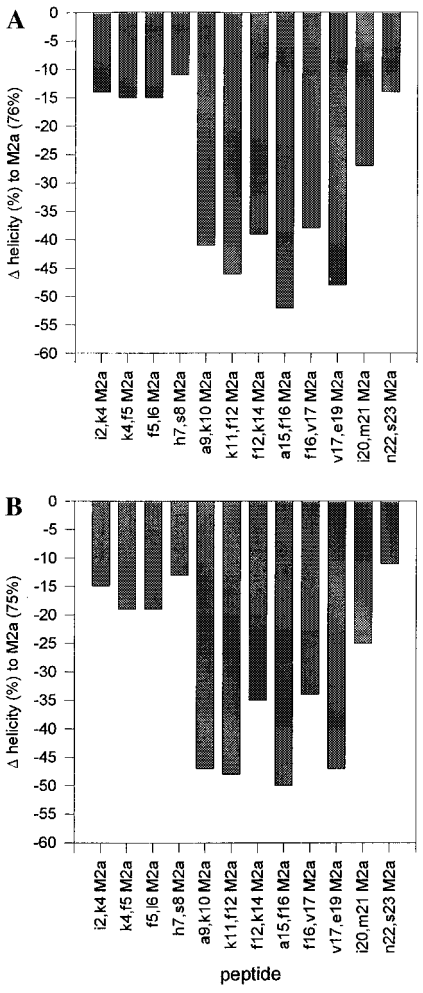

FIGURE 4: Helicity profiles of the double-D-amino acid-substituted M2a analogs (change of helicity compared to M2a) bound to phospholipid vesicles at 23 °C. (A) POPG SUVs: 13.0 mM POPG, 50 μM peptide in buffer [10 mM Tris, 154 mM NaF, and 0.1 mM EDTA (pH 7.4)]. Under these conditions, more than 99% of the peptide is in the lipid-bound state. (B) POPC/POPG (3:1) SUVs: 13.7 mM lipid, 25 μM peptide in buffer [10 mM Tris, 154 mM NaF, and 0.1 mM EDTA (pH 7.4)]. Under these conditions, more than 95% of the peptide is in the lipid-bound state.

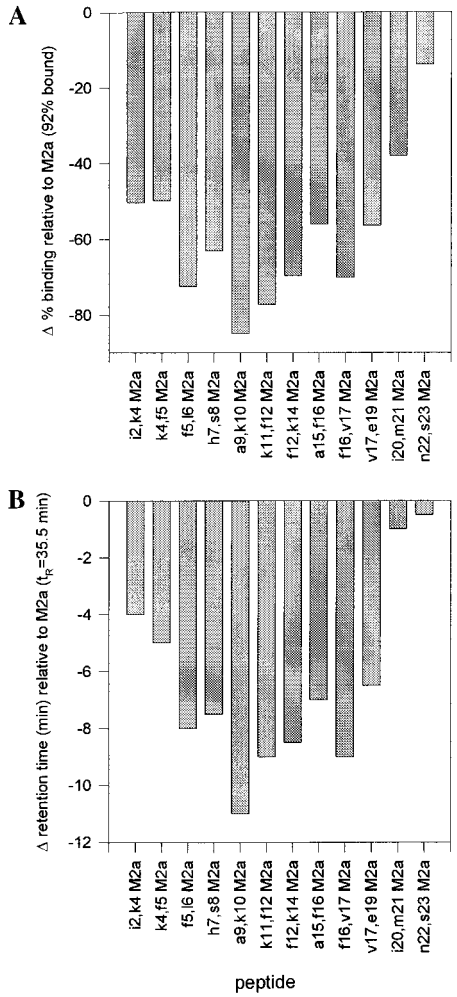

FIGURE 5: (A) Change in the POPC-bound peptide fraction (X_{bound}) compared to M2a: 11.5 mM POPC, 25 μM peptide in buffer [10 mM Tris, 154 mM NaF, and 0.1 mM EDTA (pH 7.4)]. The calculation is based on the assumption that the helicity of the double D-isomers completely bound to POPC SUVs and POPC/POPG (3:1) SUVs is identical. The procedure is described in the text. (B) Change in the retention time for the double D-isomers compared to M2a (t_R = 35.5 min). For chromatographic details, see Experimental Procedures.

isomers a^9,k^{10} M2a to i^{20},m^{21} M2a. The profile confirms the existence of a weak helix in the N-terminus and a stable helical structure in the C-terminal chain region.

Membrane Permeabilization Abilities. The calcein-releasing abilities of M2a and the double D-isomers from POPC/POPG (3:1) LUVs and POPG LUVs are illustrated in panels A and B of Figure 7, respectively. All double D-isomers exhibit a dramatic loss in their ability to permeabilize POPC/POPG (3:1) membranes compared with the all-L-amino acid peptide, indicating that the entire peptide structure is required for permeabilization of these membranes. The EC_{25} values of dye release (peptide concentrations at 25% dye release after 1 min) from POPC/POPG (3:1) vesicles for M2a and representative double-D-isomers (Table 4) reveal that double-D-amino acid substitution in the weak helix region leads to a 10-fold decrease in the ability to permeabilize membranes (see k^4,f^5 M2a), whereas substitution in the strong helix

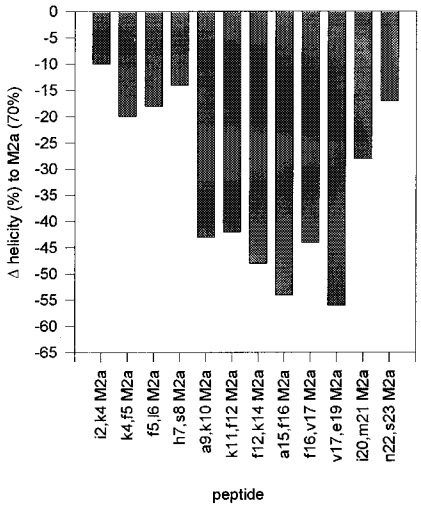

FIGURE 6: Helicity profiles of the double-D-amino acid replacement set (change of helicity compared to M2a) in the presence of SDS micelles: 25 mM SDS, 25 μM peptide in buffer [10 mM Tris, 154 mM NaF, and 0.1 mM EDTA (pH 7.4)].

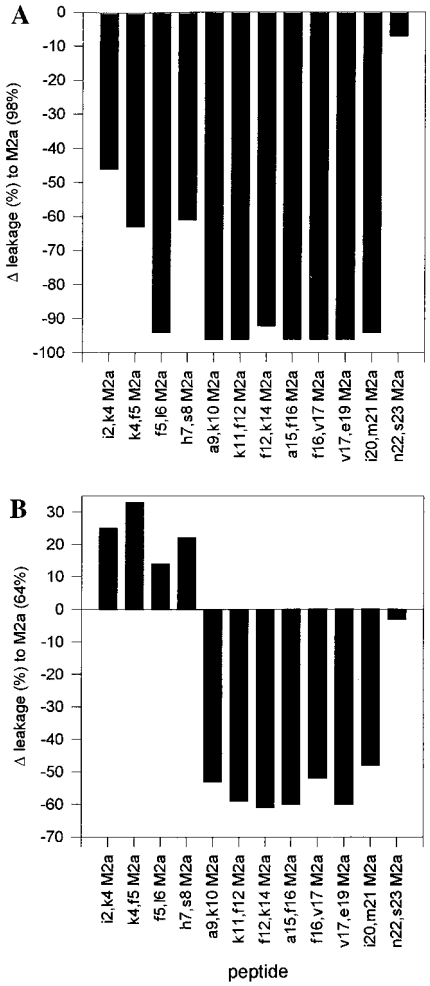

FIGURE 7: Change in the initial rate of peptide-induced calcein leakage (percent leakage for the initial minute) out of dye-entrapped LUVs relative to M2a. (A) Leakage out of POPC/POPG (3:1) LUVs: 25 μM lipid, 16 μM peptide in buffer [10 mM Tris, 154 mM NaCl, and 0.1 mM EDTA (pH 7.4)]. (B) Leakage out of POPG LUVs: 25 μM lipid, 0.3 μM peptide in buffer [10 mM Tris, 154 mM NaCl, and 0.1 mM EDTA (pH 7.4)]. Results are the mean of two independent measures, which deviate not more than 5%.

region practically inactivates the peptide (e.g. k^{11},f^{12} M2a and f^{16},v^{17} M2a).

Table 4: EC_{25} and EC_{50} Values of Dye Release (after 1 min) from POPC/POPG (3:1) and POPG LUVs for M2a and Representative Double D-Isomers[a]

peptide	POPC/POPG (3:1) EC_{25} (μM)[b]	POPG EC_{50} (μM)
M2a	1.65 ± 0.05	0.26 ± 0.02
k^4,f^5 M2a	14 ± 1	0.18 ± 0.02
k^{11},f^{12} M2a	—[c]	0.52 ± 0.03
f^{16},v^{17} M2a	—[c]	0.40 ± 0.03

[a] Dye release (after 1 min) was measured at 23 °C in buffer [10 mM Tris, 154 mM NaCl, and 0.1 mM EDTA (pH 7.4)] with a lipid concentration of 25 μM. [b] EC_{25} is shown, because EC_{50} could only be determined for M2a. [c] At the highest peptide concentration (50 μM), dye release was <5%. All values are the mean of two measurements.

In accordance with previous reports, M2a is more active in permeabilizing highly negatively charged membranes than vesicles containing high amounts of zwitterionic phospholipids [EC_{50}(POPG) = 0.26 μM, EC_{50}(POPC/POPG (3:1) = 3.0 μM]. The EC_{50} values of dye release for M2a and representative double D-isomers (Table 4) indicate that all the isomers are able to permeabilize the bilayer in a relatively narrow, submicromolar concentration range. Surprisingly, double-D-amino acid substitution up to position 8 does not reduce the activity of the peptide to permeabilize POPG LUVs, but instead, these modifications lead to an enhanced activity compared to M2a (Figure 7B). The reasons for this enhancement are at present unclear; however, it can be concluded that the weak α-helix in the N-terminal chain region is not responsible for the POPG membrane-disturbing effect of M2a. In contrast, substitution in the region of the stable helix reduces the percentage of calcein release, thus revealing the importance of this helical region for the permeabilization of POPG vesicles.

Location and Solvent Accessibility of Membrane-Bound Peptide. To examine the location and solvent accessibility of the lipid-bound helical M2a (76% α-helix on POPG SUVs), and the nearly nonhelical isomer a^{15},f^{16} M2a (24% α-helix on POPG SUVs) we determined the tryptophan fluorescence spectra of W^{16} M2a and a^{15},w^{16} M2a analogs and investigated the effect of the water-soluble quenchers iodide (I^-) and cesium ions (Cs^+). In both analogs, the phenylalanine in position 16 is substituted by tryptophan. CD experiments in the presence of vesicles did not show any differences in the conformational properties of the phenylalanine- and tryptophan-containing peptides. Furthermore, there were no changes observed in the helicity of the bound peptides after addition of 240 mM CsCl, revealing that the peptides remain completely vesicle-bound (data not shown). The fluorescence spectra of the two analogs in the POPG-bound state (curves 2 and 4 in Figure 8) show a significant blue shift of the tryptophan fluorescence maxima and an increase in the intensities compared to the spectra in buffer (curves 1 and 3 in Figure 8). The fluorescence maxima of W^{16} M2a and a^{15},w^{16} M2a were found to be at 354 and 353 nm in buffer and at 336 and 339 nm in the lipid-bound state, respectively. These spectroscopic changes point to a more hydrophobic tryptophan environment in the vesicle-bound state (Bursten et al., 1973; Lakowicz, 1983). In this environment, the accessibility of the tryptophan residues to aqueous quenchers should be reduced. The results of the quenching experiments with iodide demonstrate (Table 5) that the peptides are efficiently quenched in buffer; however, the quenching of the lipid-bound peptide is negligible. Therefore, the tryptophan residues in both

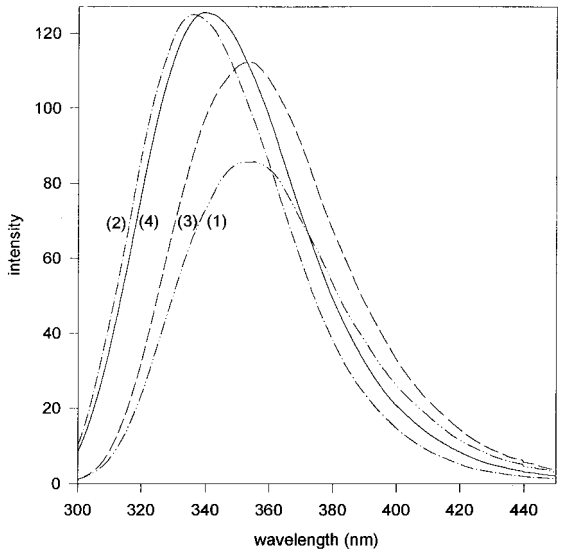

FIGURE 8: Tryptophan emission spectra of (1) W^{16} M2a in buffer [10 mM Tris, 154 mM NaCl, and 0.1 mM EDTA (pH 7.4)], (2) W^{16} M2a in a POPG SUV suspension (400 μM), (3) a^{15},w^{16} M2a in buffer [10 mM Tris, 154 mM NaCl, and 0.1 mM EDTA (pH 7.4)], and (4) a^{15},w^{16} M2a in a POPG SUV suspension (400 μM); the peptide concentration was 2 μM.

bilayer-associated peptides are shielded from the surrounding solvent. However, cesium ions were found to be effective quenchers for a fraction of about 20% of the two lipid-bound peptides (Table 5). A second larger peptide fraction of about 80% of both peptides is not accessible to cesium ions. The higher Stern−Volmer constants for the quencher-accessible fraction of bound W^{16} M2a and a^{15},w^{16} M2a (9.5 and 6.5, respectively) compared to those for the free peptides (0.94 and 1.01) can be explained by the much higher concentration of the quencher in the lipid head group region as a result of attractive electrostatic interactions between the negatively charged POPG head groups and the positively charged cesium ions.

Table 5: Comparison of the Stern−Volmer Quenching Constants of W^{16} M2a and a^{15},w^{16} M2a[a]

peptide	K_{SV} (M^{-1}) buffer[b]	POPG SUV[c]	
quenching by iodide ions			
W^{16} M2a	6.3 ± 0.5	0.0 ± 0.2	
a^{15},w^{16} M2a	7.5 ± 0.6	0.2 ± 0.2	
quenching by cesium ions			
W^{16} M2a	0.94 ± 0.05	9.5 ± 0.5 [d] fraction 1 (21 ± 2%)	0.0 ± 0.1 fraction 2 (79 ± 2%)
a^{15},w^{16} M2a	1.01 ± 0.05	6.5 ± 0.5 fraction 1 (20 ± 2%)	0.0 ± 0.1 fraction 2 (79 ± 2%)

[a] Quenching constants (K_{SV}) were evaluated from the linear Stern−Volmer plots of I^- quenching in the presence and absence of vesicles and Cs^+ quenching in the absence of vesicles according to $I_0/I = 1 + K_{SV}C_{quencher}$. All values are the means ± SD ($n = 3$). [b] 2 μM peptide in buffer [10 mM Tris, 154 mM NaF, and 0.1 mM EDTA (pH 7.4)]. [c] 2 μM peptide in 400 μM POPG SUV suspension in buffer. [d] The fractions of POPG-bound peptides (f_i) with different cesium ion accessibility and the quenching constants were evaluated from the nonlinear quenching curves by curve fitting using the equation $I/I_0 = \sum f_i/(1 + K_{SVi}C_{quencher})$ (Eftink, 1991).

DISCUSSION

The amphiphilic α-helix is believed to be an important structural feature for membrane-permeating peptides. In this work, we investigated the helical regions of magainin 2 amide bound to vesicles and in structure-inducing environments such as TFE/buffer mixtures and SDS micellar suspensions using the new method of systematic double-D-amino acid replacement of adjacent amino acids in combination with CD spectroscopy (Krause et al., 1994, 1995). Furthermore, we employed this method to locate peptide regions which are responsible for effective membrane permeabilization.

Liposomes are lipid bilayer systems comparable to lipid matrices of biomembranes and are therefore suitable systems to study the membrane active secondary structure of peptides. It has been shown that the membrane activity of magainins is modulated by electrostatic interactions of charged and polar peptide groups with the head groups of the phospholipids and by hydrophobic interactions of the nonpolar residues with the acyl chains of the lipids (Matsuzaki et al., 1991; Bechinger et al., 1993). While electrostatic interactions appear to modulate accumulation of the peptide at the bilayer surface, hydrophobic interactions have been found to drive insertion into the nonpolar membrane region (Matsuzaki et al., 1989, 1991, 1995b; Vaz Gomes et al., 1993). It is possible to modulate the electrostatic interaction term and to study its influence on peptide secondary structure by changing the amount of negatively charged phospholipid (POPG). A prerequisite for investigation of the structure of the membrane-associated peptide is its almost complete binding. Conditions allowing more than 95% of peptide bound to negatively charged POPG and POPC/POPG (3:1) vesicles were calculated from binding isotherms of M2a and representative double D-isomers (Table 3, Figure 3). Because of the weak binding of double D-isomers to zwitterionic POPC vesicles, determination of the secondary structure of membrane-bound M2a was based on a comparison of the binding profile (reflecting the apparent binding constants) of the double D-isomers with the retention profile on a DMPC-loaded HPLC column (Figure 5). Our structural investigations reveal that M2a adopts a similar secondary structure independent of lipid composition, namely a weak helix from the N-terminus up to amino acid position 8 and a stable helix ranging from residue 9 to 21. This result is in contradiction to observations of Matsuzaki et al. (1991, 1993), who found the vesicle-bound magainin 2 to be nonhelical at the C-terminus. An explanation for the difference might be that the peptide investigated was not amidated at the C-terminus. Nevertheless, our results confirm the observations of Bechinger et al. (1993) that nearly the entire peptide is α-helical in the lipid-bound state.

The independence of the secondary structure of membrane-bound M2a of the content of negatively charged phospholipids points to the conclusions that (i) differences of the affinity of peptide for lipid systems with different negative surface charges are not caused by structural differences of the lipid-bound peptide and (ii) the stabilization of the secondary structure of the membrane-bound peptide is not dominated by electrostatic interactions. Conformational differences reported for magainins in the presence of vesicles of different surface charges seem rather to be due to incomplete membrane binding of the peptide and different sample preparation methods (Duclohier et al., 1989; Jackson et al., 1992; Bechinger et al., 1993). Moreover, varying helicities

may also be caused by differences in the fluidity of the lipid bilayer (Williams et al., 1990; Jackson et al., 1992).

Double-D-amino acid substitution in the center of the stable helix leads to a drastic reduction in helicity from about 75 to about 25% (see Figure 4). Fluorescence investigations of tryptophan analogs of M2a and a^{15},f^{16} M2a should clarify whether the pronounced differences in helicity are correlated with differences in insertion of the peptides in the lipid bilayer and in their shielding from the aqueous solution. The blue shift in the tryptophan emission spectra of POPG-bound W^{16} M2a and less helical a^{15},w^{16} M2a as well as the Stern−Volmer constants are comparable (Table 5, Figure 8). Hence, significant differences in the tryptophan location do not exist. Because the anionic quencher iodide was found to be ineffective in quenching the fluorescence of the POPG-bound peptides, we conclude that the chromophores of both peptides are either penetrated into the bilayer or localized at the bilayer surface where the iodide concentration is reduced due to electrostatic repulsion. Surprisingly, also in the presence of cesium ions, which should be accumulated in the negatively charged POPG head group region, but should not be allowed to penetrate the acyl chain region, the two peptides show almost identical properties (Table 5). The nonlinear Stern−Volmer plots of the lipid-bound peptides (not shown) point to the existence of peptide fractions with a different accessibility to cesium ions. The analysis shows that a major fraction of about 80% is not accessible to the ions whereas a minor fraction of about 20% of both peptides is exposed to the quencher. Hence, the tryptophan residues of the majority of the two peptides immerse into the lipid acyl chain region, as recently reported for magainin 2 (Matsuzaki et al., 1994). In contrast, the chromophores of the minor fractions are located in the lipid head group region where the cesium ion concentration is enhanced, thus causing comparably high Stern−Volmer constants (Table 5). On the basis of these experiments, it is impossible to decide whether the existence of the two different peptide fractions results from different binding places in the bilayer or from a fast exchange of the peptides between the bilayer surface and acyl chain region.

TFE/water mixtures and SDS micellar solutions are often used to mimic membrane environments (Marion et al., 1988; Rizo et al., 1993; Chupin et al., 1995; Franklin et al., 1994; Gilbert & Baleja, 1995). Investigations of the double-D-amino acid replacement set in a TFE/buffer solution (1:1, v/v) have shown that M2a should be helical over the entire peptide chain as reflected by the relatively uniform reduction in helicity observed for all double D-isomers (Figure 2A). In contrast, only about 50% helicity was calculated from the CD spectrum of M2a (Figure 1). These observations clearly illustrate the limits of the application of CD spectroscopy for small, flexible peptides, since the latter result does not allow one to decide whether only 50% of the residues are in a helical conformation or if the reduced helicity is due to high flexibility of the completely helical peptide. However, comparison of the evaluated helicity of M2a with the helicity profile of the double D-isomers (Figure 2A) allows the conclusion that at room temperature M2a forms a less stabilized helix along the entire peptide chain. This conclusion is reinforced by the observation that a reduction in temperature stabilizes the magainin helix as indicated by higher helicity and a more pronounced and differentiated helicity profile for the double-D-amino acid replacement set (Figure 2B). However, we did not find helical regions with a different stability at room temperature. These results are in general agreement with the ^{1}H NMR results of Marion et al. (1988), who reported that in 25% TFE all the NH−NH (i, i+1) NOEs were found but only some of the CHα−NH (*i*, *i*+3) NOEs, which are characteristic of helical structures, could be observed. By comparison of the structural differences between M2a bound to liposomes and in TFE solution, it can be concluded that TFE is not well-suited for investigation of conformational aspects of magainin−membrane interactions.

SDS micelles are amphiphilic structures comparable to liposomes (Tanford & Reynolds, 1976) but have a higher curvature and a nonaqueous interior. The investigations of M2a and the double-D-amino acid replacement set clearly demonstrate that significant differences in secondary structure of M2a bound to liposomes or micelles do not exist (compare Figures 4 and 6). The SDS-bound M2a is also characterized by a weak helix up to position 8 and a stable helix between positions 9 and 21. Clearly, detergent micelles seem to be well-suited for determination of the secondary structure of membrane-bound magainin. These results confirm FT-IR observations by Jackson et al. (1992) but are in conflict with results of Williams et al. (1990), which showed that the Raman spectra of M2a bound to vesicles or to SDS micelles are different. Probably the spectroscopic differences in the latter work are caused by the very low SDS:peptide ratio (1.5 by weight), resulting in incomplete micelle binding of the peptide.

To study the role of peptide regions for membrane permeabilization, we investigated the ability of M2a and the double D-isomers to release dye from vesicles. Double-D-amino acid substitution at any position significantly decreases the dye-releasing activity on liposomes of reduced negative charge density POPC/POPG (3:1) (Figure 7A). This result can be explained by the much lower binding affinity of the double D-isomers compared to the all-L-peptide (see binding isotherms, Figure 3; binding constants, Table 3). We suggest that the different affinity of the analogs to vesicles bearing a low negative charge is caused by the fact that hydrophobic peptide−lipid interactions become effective. Double-D-amino acid substitution decreases helicity and leads to a reduction of the hydrophobic surface area of the peptide. Consequently, hydrophobic interactions between the nonpolar face of the peptides and the acyl chains of the phospholipids will be reduced in the double D-isomers. The about 50 times higher binding affinity of the peptides to POPC/POPG (3:1) compared to that to the electrically neutral POPC system (Table 3) illustrates the remaining contribution of electrostatic interactions.

In contrast, double-D-amino acid replacement only in the region of the strong helix decreases the releasing activity on highly negatively charged POPG vesicles, whereas analogs substituted up to position 8 do not reduce dye release (Figure 7B). In conclusion, the stable helix between positions 9 and 21 appears to be the main conformational feature responsible for the disturbance of POPG membranes. These results are in general agreement with the finding that removal of the first three residues from the N-terminus (weak helix region) only slightly affects the antibacterial activity of magainin, whereas deletion of only one residue from the C-terminus (strong helix region) leads to a substantial loss of activity (Zasloff et al., 1988). The observation of the

authors that removal of the cationic lysine residue at position 4 drastically reduces antimicrobial activity can be associated with a change in electrostatic interactions. Nevertheless, despite their reduced helicity, the double D-isomers and M2a permeabilize the POPG membrane in a relatively narrow concentration range (compare the EC_{50} at POPG and EC_{25} at mixed vesicles, Table 4). This fact and the higher binding constants of M2a and the double D-isomers to POPG vesicles compared to that of POPC/POPG (3:1) vesicles (Table 3) strongly suggest that binding to POPG vesicles is dominated by electrostatic interactions. Disturbance of the amphiphilic helix by double-D-amino acid substitution does not inactivate the peptide. This suggests also that peptides with a very low helicity can significantly disturb bilayers with a high negative surface charge.

Systematic double-D-amino acid replacement of adjacent amino acids has been shown to be a suitable tool to study the α-helical regions of a membrane-bound peptide. The advantage of combining systematic chemical peptide modification with CD spectroscopy is that, in contrast to conventional optical spectroscopic methods, conclusions may be drawn not only about the overall content of secondary structure elements but also about the secondary structure around individual amino acid positions. For the investigation of the structure of peptides bound to liposomes, this method exceeds at present the opportunities of two-dimensional ^{1}H NMR. The limiting factors in this method are the problems encountered when the synthesis of longer peptides is necessary and difficulties in interpreting conformational changes in double D-isomers of peptides which form more complex secondary structures.

In summary, our data reveal that lipid-bound M2a adopts an α-helical conformation which is widely independent of the content of negatively charged phospholipids. The magainin helix is characterized by a weak helix region comprising residues 1−8 and a well-stabilized helix between residues 9 and 21. Whereas only a disturbance of the strong helix reduces activity on negatively charged POPG vesicles, double-D-amino acid substitution at each position decreases the permeabilization effect on vesicles having a reduced negative charge density [POPC/POPG (3:1)]. The activity of M2a and the less helical analogs on POPG liposomes was found to be determined predominately by electrostatic interactions, while that on POPC/POPG (3:1) vesicles is characterized by a substantial contribution of hydrophobic interactions between the amphiphilic helix and the lipid acyl chains.

ACKNOWLEDGMENT

We thank A. Klose, D. Smettan, B. Pisarz, and H. Nikolenko for technical assistance and L. A. Carpino for critical reading of the manuscript.

REFERENCES

Bechinger, B., Zasloff, M., & Opella, S. J. (1993) *Protein Sci. 2*, 2077−2084.
Bessalle, R., Haas, H., Goria, A., Shalit, I., & Fridkin, M. (1992) *Antimicrob. Agents Chemother. 36*, 313−317.
Beyermann, M., Wenschuh, H., Henklein, P., & Bienert, M. (1992) in *Innovation and Perspectives in Solid Phase Synthesis* (Epton, R., Ed.) pp 349−353, Intercept Ltd., Andover.
Böttcher, C. J. F., van Gent, C. M., & Pries, C. (1961) *Anal. Chim. Acta 24*, 203−204.
Bursten, E. A., Vendenkina, N. S., & Ivkova, M. N. (1973) *Photochem. Photobiol. 18*, 263−279.
Chakrabartty, A., Schellmann, J. A., & Baldwin, R. L. (1991) *Nature 351*, 586−588.
Chen, H.-C., Brown, J. H., Morell, J. L., & Huang, C. M. (1988) *FEBS Lett. 236*, 462−466.
Chen, Y. H., Yang, J. T., & Martinez, H. M. (1972) *Biochemistry 11*, 4120−4131.
Chupin, V., Killian, J. A., Breg, J., de Jongh, H. H. J., Boelens, R., Kaptein, R., & de Kruijff, B. (1995) *Biochemistry 34*, 11617−11624.
Cruciani, R. A., Barker, J. L., Durell, S. R., Raghunathan, G., Guy, H. R., Zasloff, M., & Stanley, E. F. (1992) *Eur. J. Pharmacol. 226*, 287−296.
Duclohier, H., Molle, G., & Spach, G. (1989) *Biophys. J. 56*, 1017−1021.
Eftink, M. R. (1991) in *Methodes in Biochemical Analysis* (Suelter, C. H., Ed.) pp 127−205, John Wiley & Sons, New York.
Fairman, R., Anthony-Cahill, S. P., & DeGrado, W. F. (1992) *J. Am. Chem. Soc. 114*, 5458−5459.
Franklin, J. C., Ellena, J. F., Jayasinghe, S., Kelsh, L. P., & Cafiso, D. S. (1994) *Biochemistry 33*, 4036−4045.
Gilbert, G. E., & Baleja, J. D. (1995) *Biochemistry 34*, 3022−3031.
Grant, E., Jr., Beeler, T. J., Taylor, K. M. P., Gable, K., & Roseman, M. A. (1992) *Biochemistry 31*, 9912−9918.
Hope, M. J., Bally, M. B., Webb, G., & Cullis, P. R. (1985) *Biochim. Biophys. Acta 812*, 55−65.
Jackson, M., Mantsch, H. H., & Spencer, J. H. (1992) *Biochemistry 31*, 7289−7293.
Juretic, D., Hendler, R. W., Kamp, F., Caughey, W. S., Zasloff, M., & Westerhoff, H. V. (1994) *Biochemistry 33*, 4562−4570.
Krause, E., Beyermann, M., Dathe, M., Wenschuh, H., Rothemund, S., & Bienert, M. (1994) in *Peptides: Chemistry, Structure and Biology* (Hodges, R. S., & Smith, J. A., Eds.) pp 247−248, Escom Science, Leiden, The Netherlands.
Krause, E., Beyermann, M., Dathe, M., Rothemund, S., & Bienert, M. (1995) *Anal. Chem. 67*, 252−258.
Lakowicz, J. R. (1983) *Principles of Fluorescence Spectroscopy*, Plenum Press, New York.
Marion, D., Zasloff, M., & Bax, A. (1988) *FEBS Lett. 227*, 21−26.
Matsuzaki, K., Harada, M., Handa, T., Funakoshi, S., Fujii, N., Yajima, H., & Miyajima, K. (1989) *Biochim. Biophys. Acta 981*, 130−134.
Matsuzaki, K., Harada, M., Funakoshi, S., Fujii, N., & Miyajima, K. (1991) *Biochim. Biophys. Acta 1063*, 162−170.
Matsuzaki, K., Murase, O., Funakoshi, S., Fujii, N., & Miyajima, K. (1993) in *Peptide Chemistry* (Yanaihara, N., Ed.) pp 691−693, ESCOM, Leiden, The Netherlands.
Matsuzaki, K., Murase, O., Tokuda, H., Funakoshi, S., Fujii, N., & Miyajima, K. (1994) *Biochemistry 33*, 3342−3349.
Matsuzaki, K., Murase, O., Fujii, N., & Miyajima, K. (1995a) *Biochemistry 34*, 6521−6526.
Matsuzaki, K., Sugishita, K., Fujii, N., & Miyajima, K. (1995b) *Biochemistry 34*, 3423−3429.
Pouny, Y., & Shai, Y. (1992) *Biochemistry 31*, 9482−9490.
Provencher, S. W. (1982) *Comp. Phys. Commun. 27*, 213−227.
Rizo, J., Blanco, F. J., Kobe, B., Bruch, M. D., & Gierasch, L. M. (1993) *Biochemistry 32*, 4881−4894.
Rothemund, S., Krause, E., Beyermann, M., Dathe, M., Engelhardt, H., & Bienert, M. (1995) *J. Chromatogr., A 689*, 219−226.
Schwarz, G., & Beschiaschvili, G. (1989) *Biochim. Biophys. Acta 979*, 82−90.
Soravia, E., Martini, G., & Zasloff, M. (1988) *FEBS Lett. 228*, 337−340.
Tanford, C., & Reynolds, J. A. (1976) *Biochim. Biophys. Acta 457*, 131−170.
Vaz Gomes, A., de Waal, A., Berden, J. A., & Westerhoff, H. V. (1993) *Biochemistry 32*, 5365−5372.
Westerhoff, H. V., Juretic, D., Hendler, R. W., & Zasloff, M. (1989) *Proc. Natl. Acad. Sci. U.S.A. 86*, 6597−6601.
Williams, R. W., Starman, R., Taylor, K. M. P., Gable, K., Beeler, T., Zasloff, M., & Covell, D. (1990) *Biochemistry 29*, 4490−4496.
Zasloff, M. (1987) *Proc. Natl. Acad. Sci. U.S.A. 84*, 5449−5453.
Zasloff, M., Martin, B., & Chen, H.-C. (1988) *Proc. Natl. Acad. Sci. U.S.A. 85*, 910−913.

BI960362C